Heliyon 6 (2020) e05570

Contents lists available at ScienceDirect

Heliyon

journal homepage: www.cell.com/heliyon

Research article

Spatial attention modulates earliest visual processing: An electrical neuroimaging study

Alberto Zani [a,c,*], Alice Mado Proverbio [b,c]

[a] School of Psychology, Vita Salute San Raffaele University, Milan, Italy
[b] Department of Psychology, University of Milano-Bicocca, Milan, Italy
[c] Neuro-Mi Center for Neuroscience, University of Milano-Bicocca, Milan, Italy

ARTICLE INFO

Keywords:
Cognitive neuroscience
Visuospatial orienting of attention
Preparatory bias
Spatial anisotropy
Early attentional selection
ERPs
Intracranial source reconstruction
High temporal and spatial localization resolution
Striate occipital cortex
Extrastriate occipital cortex
Behavioral test
Nervous system
Cognition
Systems neuroscience
Neuroanatomy
Cognitive psychology

ABSTRACT

Several studies showed that shifting of visuospatial attention modulates sensory processing at multiple levels of the visual pathways and beyond, including the occipital striate cortices level. However, inconsistent findings have been reported thus leaving these issues still disputed. 21 participants took part to the present study (the EEG signals of 4 of them were discarded due to artifacts). We used ERPs and their neural sources to investigate whether shifting spatial attention in space across the horizontal meridian of the visual field affected striate cortices activation at the earliest latency. Time-series of scalp topographical maps indicated that, unlike ERPs to attentional-neutral central cues, ERPs to attention-directing local cues showed earliest polarity inversions as a function of stimulated field and processing latency range considered, at occipital-parietal electrodes. In between 60-75 ms, attentional shifting cues elicited a positivity for both visual fields, whereas at a later latency (75–90 ms) they elicited a positivity and a negativity for the upper and lower visual hemifields, respectively. Computed neural sources included striate, besides extrastriate, cortices for both visual hemifields and latency ranges. Conjointly, behavioral responses to targets were faster when they were preceded by local than by neutral cues, and when presented in the upper than the lower hemifield. Our findings support the hypothesis that attention shifts may affect early sensory processing in visual cortices.

1. Introduction

Functional neuroimaging of brain attentional networks has been so successful to be able to reveal much more than simply the locus of visual attentional selection in the brain [1]. Indeed, thanks to the new insights provided, current models postulate that neural mechanisms of selective information processing are part of a multilevel selection system spanning from the subcortical thalamic regions up to the higher-order fronto--parietal cortices, with in between the occipital striate and extrastriate cortices, each one playing a different filtering role [2, 3].

Notwithstanding these new insights, controversial findings about the neuroanatomical localization and/or temporal progression of selective processing of visual information through the levels of the visual attention system have been reported in the literature. Before presenting a review of findings against and in favor of these earlier or later attentional effects as a function of resolution features of imaging methods utilized, both singularly or in combination with each other (e.g., ERPs and fMRI), it can be useful to illustrate summarily the common features characterizing the many studies from which these findings are drawn. Indeed, these inconsistent findings concern both the response to cue and/or target stimuli in typical cue-target spatial attention orienting paradigms. Despite the variants of these paradigms, the typical structure consists in the presentation of an attentional cue, a stimulus followed after a variable time delay, depending on the imaging method, by the presentation of a target, i.e., a stimulus requiring a behavioral response, at either the cued location (i.e., cued or valid targets) or an uncued location (i.e., uncued or invalid targets.) Any neural response or overt performance benefits (e.g., a fMRI activation and/or greater ERPs as well as a motor response facilitation) for cued targets are attributed to the cue's ability to direct attention, with the time course of attentional orienting effects revealed by the change in the processing profile across the cue-target

* Corresponding author.
E-mail address: zani.alberto@hsr.it (A. Zani).

https://doi.org/10.1016/j.heliyon.2020.e05570
Received 15 January 2020; Received in revised form 3 June 2020; Accepted 18 November 2020

intervals [4]. Below a thorough review of these hemodynamic and ERP findings shall be presented.

As for hemodynamic studies based on these cue-target spatial attention tasks, a modulation of the (V1) striate, besides of extrastriate, visual cortex [5, 6, 7, 8] and of the earlier level thalamic pulvinar [9] (La Berge and Buchsbaum, 1990) as well as of the lateral geniculate nucleus (LGN) [8, 10, 11] processing of targets were reported by several fMRI studies. Such a modulation has been also found in response to attention orienting cues in the absence of target delivery [8, 12]. This modulation of visual cortex and earlier structures of the visual system activity in response to attention orienting cues has been interpreted as a "*preparatory bias*" induced by top-down signals from higher-levels brain areas, which has been reported to be dissociated from target attentional processing [13]. Hopfinger *et al.* (2000) [14] recorded event-related fMRI responses of visual cortices to both targets and prior cues signalling their locations separated by an 8-s time gap. They found indications of an activation of the contralateral visual sensory regions in response to both targets and cues, including V1. Hence, they argued that, unlike reflecting an enhanced target processing induced by focused spatial attention, the enhanced activity in visual sensory cortices related to the orienting cues was a reflection of a preparatory biasing of these cortices due to top-down modulation.

Since hemodynamic signals have a limited temporal resolution, fMRI is unable *per se* to provide information on the parallel and sequential activation of brain areas found to be related to the selective processing. However, the recording of high-time resolution electrical and magnetic signals (i. e., ERPs and MEG) in humans has originally provided compelling evidence of the timing of attentional selection of visual information at P1 and N1 longer-latency sensory responses of the visual cortex in between 70 and 200 ms post-stimulus for target processing [15].

The combining of ERP recordings with hemodynamic measures in humans provided evidence of an activation of the fusiform gyrus of extrastriate cortex, which was proposed to be the neural counterpart of the P1 time-related attentional modulation [16]. In addition, fMRI evidence of a modulation of extrastriate, but not striate visual cortices, at about 70–75 ms P1-centered latency was also provided by Martinez *et al.* [17]. Any evidence of an earliest attentional modulation of the initial afferent sensory volley to the striate visual cortex was denied by this study based on the findings of an fMRI activation of V1 not being associated with a change of C1, the ERPs component that appears prior to the P1 and reflects the earliest afferent sensory volley of visual inputs to the primary occipital regions. The neural source in the calcarine fissure of the striate cortex of this component as originally theoretically advanced by Jeffreys and Axford [18] was formerly confirmed by Clark and Hillyard [19] and, later-on, reiterated by many other research groups. This striate-centred component is also referred to as P-N80 in the literature because of its 80 ms average latency and of its sensitivity to retinal stimulation coordinates, which shows as an inversion in polarity as a function of a lateralized stimulation across the visual horizontal meridian [17, 18, 19, 20, 21, 22, 23]. Indeed, C1 response shows almost invariably a negative or a less positive voltage measure in response to upper field stimuli and reverses in polarity or reaches a less negative voltage in response to lower field stimuli [19, 24, 25, 26].

Unlike this robust retino-cortical crossed visual model, when stimuli are presented along the vertical meridian an opposite trend (i. e., positive for the stimulation of the upper visual field (VF) and negative for the lower VF) was found by many studies [19, 21, 22, 27, 28]. In a recent ERP and source analysis study by Capilla *et al.* [29], this inverted response, which has been defined as a C2 component, showed an origin from the confluence of V1 and V2, where this meridian has been proposed to be mostly represented [30, 31]. That this activity is generated outside the calcarine fissure, as V2, is also supported by the uncovering that its scalp reflection and timing closely parallels the one predicted for V2 [32].

As for the effects of spatially focused attention on C1 response to target stimuli, several initial ERP studies failed to show any significant findings [20, 27, 33, 34]. However, evidence has accumulated over time (e. g., see Zhang et al. [35], for a review of this evidence) suggesting that spatial attention directly affect striate cortex as reflected by an active modulation of the C1 component. For instance, evidence of a robust enhancement at C1 level elicited by voluntary orienting of spatial attention has been reported using a cuing task in which standard and target stimuli were presented either at relevant or irrelevant locations across the upper and lower visual fields (see ref. [21, 36, 37, 38]). These attention effects, which were consistent across the horizontal meridian of the visual field, were attributed by source analyses to neuronal generators in the occipital striate cortex. Further evidence of a lower C1 negativity (i. e., greater positivity) under high attentional load for distracters in the upper, but not in the lower, visual hemifield during a voluntary attention task has also been reported by Rauss *et al.* [39]. Again, Fu *et al.* [40, 41] found that the combination of an involuntary, reflexive allocation of visual attention and of high perceptual load positively contributed to the earliest C1-related modulation of the striate cortex.

Strong support for an earliest visual spatial attention effect on the striate occipital cortex has been also offered by single-unit measurements [42, 43, 44]. Most importantly, these measures also indicated that this attention mode boosted the activation of the sub-cortical, thalamic lateral geniculate nucleus (LGN) and suppressed the activation of the adjacent reticular nucleus (TRN) [45]. This would be bound to a fine tuning of communication of the LGN neurons at the synaptic level by selectively increasing the efficacy of presynaptic input for driving postsynaptic responses [46].

Despite this gathering of separate and combined multi-technique-based evidence of a spatial selection already operating at sub-cortical, thalamic level, the issue of attentional effects in V1 still remains controversial with several authors arguing the earliest stages of visual cortical processing are absolutely not affected by spatial attention (e.g., see ref [47, 48]) and others adopting contrasting viewpoints that these stages might, indeed, be affected as a function of the experimental conditions used (see, e. g., the recent commentaries-crossmarked review in ref. [49]).

While the most of spatial attention research dealt with the modulation of neural processing of valid targets falling at the location indicated by cues (inducing orienting of spatial attention to that location), only a scant number of studies coped with the time course of modulation of neural responses elicited by pre-target attention-directing (or attention-shifting) cues as reflected by ERPs recorded in the processing profile across the cue-target time span. For instance, Yamaguchi et al. (1994) [50] reported that central cues elicited negative ERPs shifts starting 240 ms after cue onset over posterior scalp sites contralateral to the cued visual field. Conversely, peripheral cues enhanced an N1 component (i.e., 140–200 ms post cue) over the contralateral hemisphere. Following N1 enhancement, a sustained negative potential shift appeared after 400 ms post cue at posterior scalp sites contralateral to cued visual field. The results by other studies reinforce the notion that early response anticipation and preparation – or biasing – processes of the posterior-parietal cortex, perhaps in an the initial step of attentional orienting, are triggered by the spatial cueing stimuli, together with a later lateral-prefrontal cortex involvement, possibly related to the voluntary control and maintenance of attentional shift [50, 51, 52, 53]). However, some later studies combining ERPs and fMRI indices showed that "attending" and "interpreting" a centrally presented instructional cue (i.e., a cue instructing to shift attention to the right or left location) elicited similar sensory processing activity in the first 350 ms at occipital extrastriate areas, followed by a long-lasting negative variation, defined by the authors as a *biasing-related negativity* (BRN), over higher-levels brain areas induced by attending cues only [54, 55].

In the light of the scantiness of knowledge on occipital-parietal preparatory biasing processes induced by cue signals, the present study was aimed at further investigating cue-related visuospatial attentional shifting mechanisms and their neural mechanisms. ERP recordings and source reconstruction methods were used to investigate whether: (1) cues

directing attention to a point in space induced an earliest attentional biasing or sensory processing tuning, reflected at the scalp by a modulation of the earliest-latency C1 response to these cues; (2) this sensory tuning directly originated in the striate occipital regions of the visual system; and (3) the origins and polarity-inversion trend of C1 component differed from those of the slightly longer-latency C2 component.

Overall, the aim of the study was to assess the effects of attention on sensory potentials, by considering whether the attentional conditions and the visual field of stimulation were able to differentially modulate the amplitude of the evoked responses. Had the alertness or the attention allocation enhanced the evoked response, this would have suggested a very early attentional sensory processing. In order to gain fine-tuned temporal information, sensory potentials were analyzed every 5 ms time from 60 to 90 ms at C1 and C2 levels.

2. Methods

2.1. Ethical approval, methods accordance and informed consent

The study was approved by the ethics committee of the Italian National Research Council (CNR) and was conducted in the *Electro-Functional Brain Imaging unit* (EFBIu) of the CNR-IBFM Institute in accordance with American Psychological Association (APA) ethical standards for the treatment of human experimental participants (APA, Monitor Staff, 2003, vol. 34, n. 1). The methods were carried out in accordance with the relevant guidelines and regulations. Furthermore, the experiments were conducted with the understanding and the written consent of each participant in compliance with the indications of the 2018 Declaration of Helsinki ethical principles for medical research involving human subjects by the World Medical Association (WMA Declaration of Helsinki, 9 July 2018, PDF file).

2.2. Participants

Twenty-one participants took part to the study. The EEG data of 4 subjects were preliminarily discarded due to EEG artifacts and amplifier blocking. The EEG data of seventeen young and healthy college students (8 females and 9 males, 20–27 years old, $M = 21.43$, $SE = 3.4$ y) were analyzed. Before participating in the recording session, each of them took part in an interview scheduled by means of a college official advertisement system offering decimals of academic credits for participation in experimental projects. Accepted volunteers had to have normal or corrected–to–normal vision and right-eye as well as right-hand dominance and none of them had to have any left-handed relatives as assessed by the paper-and-pencil Edinburgh Inventory. Furthermore, none of them had to have been suffering or having suffered of any neurological and psychological disturbances or the intake of any psychopharmacological substances. Criteria of exclusion from the study were intensive cigarettes smoking, and cardiovascular and/or respiratory diseases. In addition, to minimize any performance confounding effects, all participants were asked to refrain from any strenuous physical activity in the 48 h prior to the experimental recording session. In addition, they were also required to refrain from unlimited consumption of alcohol, caffeine, and theophylline containing beverages in the same time span.

Since all the recruited volunteers showed acceptable percentages of artifactual trials, none of them was left out of final data measurements and analyses.

2.3. Stimulus materials

Stimulus materials were white arrow strings presented on the black background of a 17“ CRT remote screen placed at a distance of 114 cm (~3.34 feet) from the volunteers within an electrically and magnetically shielded, dimly lit cubicle. These strings consisted of five horizontally-contiguous arrows to which a motor response had to be given. The central arrow of each string, which might point rightward or leftward, posed as a true target. Conversely, the flanking two arrows on each side of the target arrow, which pointed toward the same (‘congruent’ flankers) or the opposite direction (‘incongruent’ flankers) as the target, posed as potential distracters. All in all, then, there were four different target-flankers combinations characterized by diverse conflicting or potential distraction-load levels (see Figure 1a; 1b, right side).

Besides arrow-strings, proper and ‘dummy’ asterisks, functioning as pre-target cues, were presented. Unlike the proper asterisks, the ‘dummy’ asterisks were of black color.

Given the blackened background of the CRT screen, unlike both the proper white asterisks and target-strings, the ‘dummy’ asterisk-cues delivered during a “no cue” task were invisible to the volunteers. At the indicated distance of 114 cm (~3.34 feet) from the volunteers, each target-flankers string subtended 8.7 degrees of visual angle (width) along the horizontal meridian and 1.3° (height at the arrow tip backside) along the vertical meridian.

Both asterisk types used subtended 0.30 degrees of visual angle. The luminance of both the proper cues and target-flanker-string types was measured in candela/m^2. Unlike the nil luminance value of the black asterisk, the luminance of the proper asterisk amounted to 7.3 cd/m^2 (see Figure 1b, left side). Conversely, the luminance for the arrow-strings was 27.81 cd/m^2 no matter the arrow-pointing directions and target-flankers congruency (see Figure 1b, right side).

2.4. Procedure

Participants were seated in a comfortable easy chair with a high backrest within the shielded cubicle. Visual stimuli were presented to them on a CRT screen with a small white fixation cross (FC) of 0.25 degrees of visual angle in the center of its black background. During EEG active recording, separate sequences of the white arrow-strings were randomly presented above or below the FC on the screen, that is, in the upper visual field (UVF) or the lower visual fields (LVF), respectively. The central arrow of each string fell just in correspondence of the FC with an eccentricity of ±1.25 degrees of visual angle from the latter along the vertical meridian (see Figure 1a).

Each arrow-string was preceded by either a proper or a dummy cue (Figure 1b, left side). Three different spatial orienting of attention conditions were used based on a modified and readapted version of Fan's et al. [56] original Attention Network Test (ANT) (see Figure 1b, left side). Indeed, the participants had to deal with: (1) a “No cue” (NC) condition based on the presentation of a ‘dummy’ cue not visible by the volunteers. This condition should have possibly induced a long-lasting tonic alert or sustained attention state in the participants, which intermingled with the exogenously-driven spatial orienting of attention to the point in space (i. e., the UVF or the LVF) where the arrow-strings were unexpectedly presented from trial-to-trial; (2) a central cue (CC) condition based on the presentation of a ‘proper’ cue overimposed on the FC aimed at eliciting a phasic alerting response, later on followed by an exogenously-driven orienting of attention to the point in space where the target appeared (i. e., the UVF or the LVF); and (3) a spatially-centered, valid orienting condition (i. e., LC), deriving from the presentation of a proper cue in the UVF or the LVF, so to elicit a mix of a phasic alerting and of an exogenously-driven spatial orienting of attention to the point in space signaled by the cue prior to the appearance of the target at that same point (see Figure 1b, left side, again).

Participants were instructed to pay attention to the screen and to continuously gaze at the FC avoiding moving their head or their eyes either towards the vertically lateralized target-strings or, during the LC pre-cuing task, to cues. For each of the three cue-target conditions randomly administered, on each trial the participants had to evaluate the pointing direction of the central arrow (i. e., right or left), independent of the direction of the flanking-arrows (Congruent or Incongruent), and to perform a RT button-press as accurately and quickly as possible. This response had to be given with the index finger of the right or left hand continuously kept over the corresponding front button of a two-handles

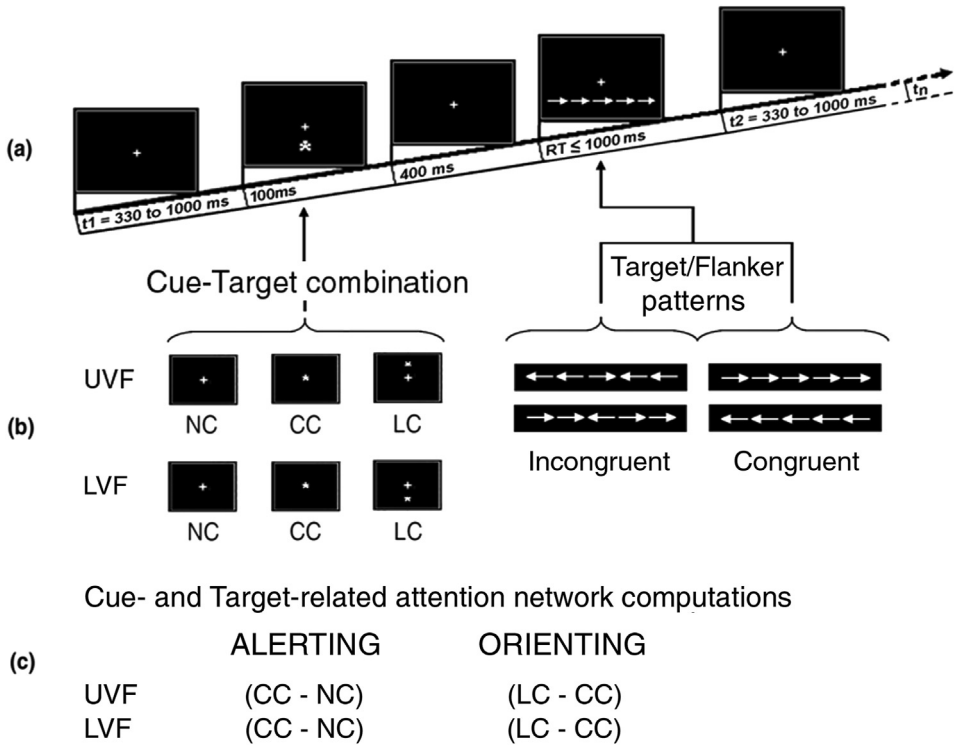

Figure 1. Schematic representation of: (a) the timing of cue and target presentation for a single example trial; (b) the different cuing and Target/Flanker pattern conditions; and (c) the computation of neural networks function.

handheld gamepad comfortably held on their lap, without looking at the buttons. To check that participants followed these instructions, both their face and eye movements were monitored through a video-camera mounted over the stimulation screen.

To familiarize participants with the task, before recording was started volunteers read detailed written instructions and performed a practice run of 30 cue-target pairs for each cuing condition.

For each cuing condition, there were four separate runs of trials, each containing 128 cue-target pairs grouped in a differently randomized order and lasting approximately 3.5 min. After each run, the volunteers received a rest period. To avoid any confounding interacting effects of practice and fatigue, we also randomized the order of administration of the cue-target conditions, of the type of target-flanker arrows, of the administration of the targets in the UVF or the LVF, and of runs presentation across participants. On each trial, the cuing asterisk appeared for 100 ms followed, after 400 ms from its offset, by the delivery of an arrows-string, which remained on the screen for 1000 ms. This was done to avoid recording any possibly baffling target-offset-related ERP. Inter-trial interval (ITI) randomly varied in between 330 and 1000 ms (see Figure 1a once again). Overall 1536 trials per participants were administered.

The ASA Lab (*Advanced Source Analysis Lab*) software package (Ver. 4.1.0.5) of *Advanced Neuro-Technologies Inc*. (A.N.T. Inc., Enschede, The Netherlands) was used for stimulus presentation and EEG data recording as well as for offline analysis and source reconstruction.

2.5. EEG recording and analysis modes

During the experimental runs, both EEG and EOG signals were recorded in continuous mode. Both these signals were amplified by means of 128-channel Average Reference Amplifiers (128-REFA), a measurement system for brain research whose electrophysiological inputs are configured as "reference" amplifier, in that all channels are amplified against the average of all connected inputs. This set-up offers significant advantages over other amplifier designs based on a common reference mode, since, unlike in the latter mode, in which a specific electrode is used as reference signal, in case of reference bad contact the average reference does not affect irreparably the signal-to-noise ratio of the electrode signals. This makes it possible to re-reference offline in software to any montage desired. The REFA is connected to a "master" PC by means of a bidirectional glass fiber. Inside the PC a fiber interface board controls the glass fiber communication and part of the data processing.

Of the 128-channels, 124 were used to record EEG signals and four to record EOG signals. The EEG electrodes were mounted in an elastic electro–cap and were located all over the scalp according to the indications specified by the 10–5 International System [57]. The labels and 3D locations of these electrodes were imported as a default set for that specific electrodes montage which was stored in the Master PC hard disk. An electrode added in the cap between Fp1 and Fp2 but 0.6 in. (i. e., 1.5 cm) below them served as a ground lead. Two of the EOG electrodes were placed below and above the right eye to record vertical eye movements (vEOG), whereas the other two electrodes were placed at the outer canthi of the eyes to record horizontal eye movements (hEOG). Both EEG and EOG signals were amplified with a half amplitude band-pass of 0.016–70 Hz. Electrode impedance was kept well below 5 kΩ. Amplifier gain for the EOG was 0.5 times that for EEG. Continuous EEGs and EOGs were digitized at a rate of 512 Hz.

Offline, automated rejection of electrical artifacts was performed before EEG averaging to discard epochs in which eye movements, blinks, amplifier blocking, or excessive motor potentials occurred. The artifact rejection criterion was a peak–to–peak amplitude exceeding +/-100 μV for EOG signals and +/– 70 μV for EEG signals. In line with the trial stimulus events timing, the artifacts monitoring routine went from 100 ms before the cue-type to 1500 ms after it for each trial in sequence, until the routine detected EEG values falling within the indicated window-values. On average, EOG artifact rejection rate was ~6.2 % whereas EEG rejected trials amounted to 10.45 % per participant. Trials associated with errors or missing (i.e., overt motor responses falling after 1000 ms from the target) were also discarded, which resulted in a rejection rate

of less the 1.21%. Overall, then, a total of 82.14% of valid trials out of the 100% trials administered were accepted for averaging. After rejection procedures and the due mean computations over the sample of participants, the mean percentages of trials accepted and averaged as a function of NC, CC, and LC conditions, out of the 82.14% of total good trials, amounted to 97.95%, 98.20%, and 99.14%, respectively. For each participant, distinct average ERP waveforms referred to linked-ears were obtained for each scalp electrode site as a function of cuing type (i. e., no cue – NC; central cue – CC; and valid spatial cue – LC) and of target presentation location (i. e., the UVF or the LVF). Indeed, due to the possible polarity inversion of the C1 response as a function of cue-stimulus retinal location across the horizontal meridian of the visual field for the valid spatial cuing condition (i. e., LC) with respect to both the CC and NC conditions, for comparison purposes we averaged separately cue-target EEG sweeps in which targets were presented in the UVF or the LVF, respectively, for all the three cuing conditions (See Figure 1c). Since the cuing conditions did not provide any information about the target-flanker arrows directional congruency (i. e., congruent or incongruent targets), trials relative to these conditions were collapsed together so to have ERPs with a greater signal-to-noise ratio. Average ERPs obtained for any of the 17 single participants were then grand–averaged across the sample.

No baseline correction across EOG and EEG waveforms was applied before averaging procedure. However, to remove any high–frequency oscillations noise, we applied an offline band-pass digital filtering in between 50 and 70 Hz to all data before their averaging and successive grand-averaging across the participants' sample. Additionally, before data measurements for comparison and displaying purposes waveforms were subjected to baseline correction over the interval from –100 ms to 0 ms.

To make sure of the spatial distribution of cue-related P/N80 (typically reaching its maximum amplitude at mesial occipital and parieto–occipital sites with respect to more lateral parietal-occipital sites, where, instead, P1 component is renown to be most prominent [19, 58], topographical voltage mapping of ERPs was performed. Time series of color-coded isopotentials and their relative contour lines were computed at intervals of 5 ms on the interpolated voltage values between posterior scalp electrodes for P/N80 (see Figure 2) as a function of the CC and LC conditions, separately for the UVF and LVF. In the same figures, the voltage mapping carried out on the difference waveforms (DW) relative to the attention orienting network described by Fan's *et al.* [56], namely, the difference between LC and CC, are also shown.

2.6. ERP measurements and statistical analyses

As clearly indicated by the time-series of the color-coded isopotentials scalp maps for P/N80 plotted in Figure 2, the focusing of maximum voltage for this component was reached at midline, posterior scalp regions, that is, at parietal (Pz), parieto-occipital (POz), occipital (Oz) and Inion (Iz) sites. However, contour lines overimposed on color-coded

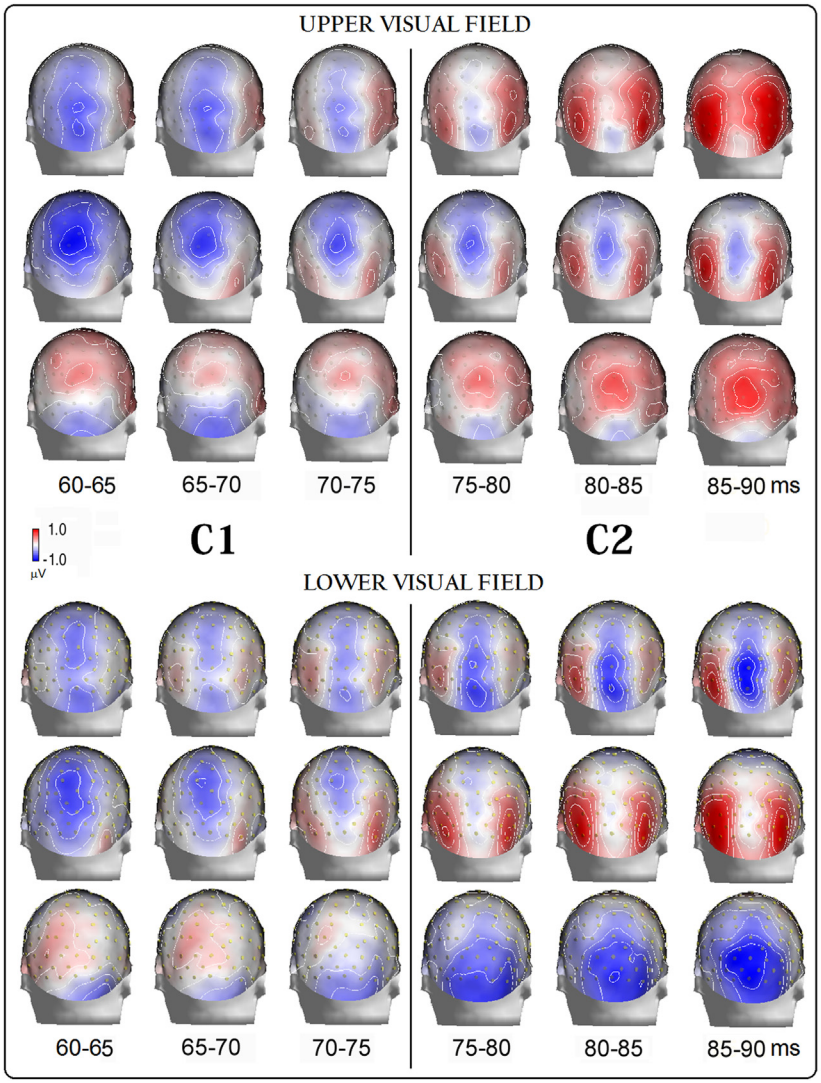

Figure 2. Time series of 3D backview color-coded and contour-lines-coded maps, plotted at intervals of 5 ms, of the earliest P/N80 voltage responses recorded within the 55–95 ms post-cue latency range as a function of LC, CC, and difference (Diff. = LC minus CC) conditions as well as of target-related visual fields (i. e., UVF and LVF). Worthy of note is that earliest post-cue voltage responses to LC present almost inverted polarity reversals and topographic distribution at occipital-parietal sites as a function of both the target-related locations (i. e., UVF and LVF) and the processing time-spans considered in between 55-75 ms and 75–95 ms. These inverted polarity reversals are consistent with those of C1 and C2 sub-components of P/N80 complex. Importantly, independent of the target-related location considered, attentional shifts were reflected at the scalp by a positivity at the earliest C1 level, and by a positivity for the UVF and a prominent negativity for the LVF, respectively, at the following C2 level.

topographic value maps indicated that mesial-occipital and lateral occipital-parietal sites were also affected by the focusing of voltage mentioned above. Brain potentials were measured where they reached their maximum amplitude at scalp surface; each piece of data underwent a single statistical analysis.

Attentional modulation displayed in the difference maps occurred at both mesial-occipital and lateral occipital-parietal sites. These findings are quite consistent with those reported in the previous literature [18, 19, 21, 23, 25, 57].

Consistent with previous literature on the C1 component, P/N80 showed a polarity conversion as a function of stimulation across the horizontal meridian of the visual field in the 60–75 ms time window [18, 19, 21, 23]. Indeed, for LC condition larger negativities (or lower positivities) can be seen to peak at the midline occipital (Oz) and inion (Iz) sites in response to the presentation of the cues in the UVF than in the LVF. Conversely, lower negativities (or larger positivities) can be seen at posterior electrode sites, especially at Oz site, in response to the cues appearing in the LVF than in the UVF (see Figure 2).

Despite these polarity changes, at C1 level the benefits of attentional modulation - as derived from the LC vs. CC contrasts – drawn in Figure 2 – always manifested at the back scalp as a greater positivity (i. e., a *source*) bilaterally distributed over parietal and parietal-occipital regions, especially for the cuing of the UVF.

As also suggested by the maps in Figure 2, while sensory processing progressed in time beyond the C1 latency range (i. e., 60–75 ms), voltage responses to LC exhibited reversed polarities with respect to the earliest time span. Indeed, higher positivities were obtained for the UVF than the LVF stimulation, and, vice versa larger negativities for the LVF than the UVF stimulation, consistent with the proposed trend for the so called C2 component [27, 29]. Most interestingly, at this relatively longer latency of processing (i. e., 75–90 ms), the attentional tuning manifested either as a positive or a negative polarity when cuing the UVF or LVF, respectively.

To investigate the data displayed in the voltage maps of Figure 2, P/N80 mean values were quantified within the two time windows of 60–75 ms (C1) and 75–90 ms (C2), respectively, as a function of the three cuing conditions (i. e., CC, LC and NC) with reference to the baseline-corrected voltage average over the interval from –100 ms to 0 ms. Based on the 512 Hz sampling rate, mean amplitude values for both C1 and C2 time windows were obtained averaging 8 data points, corresponding to an EEG sweep time-span of 16 ms, for each of the 17 participants.

Measurements were carried out at the sites where ERPs voltage reached their maximum amplitude, i. e., over parietal (Pz), parieto-

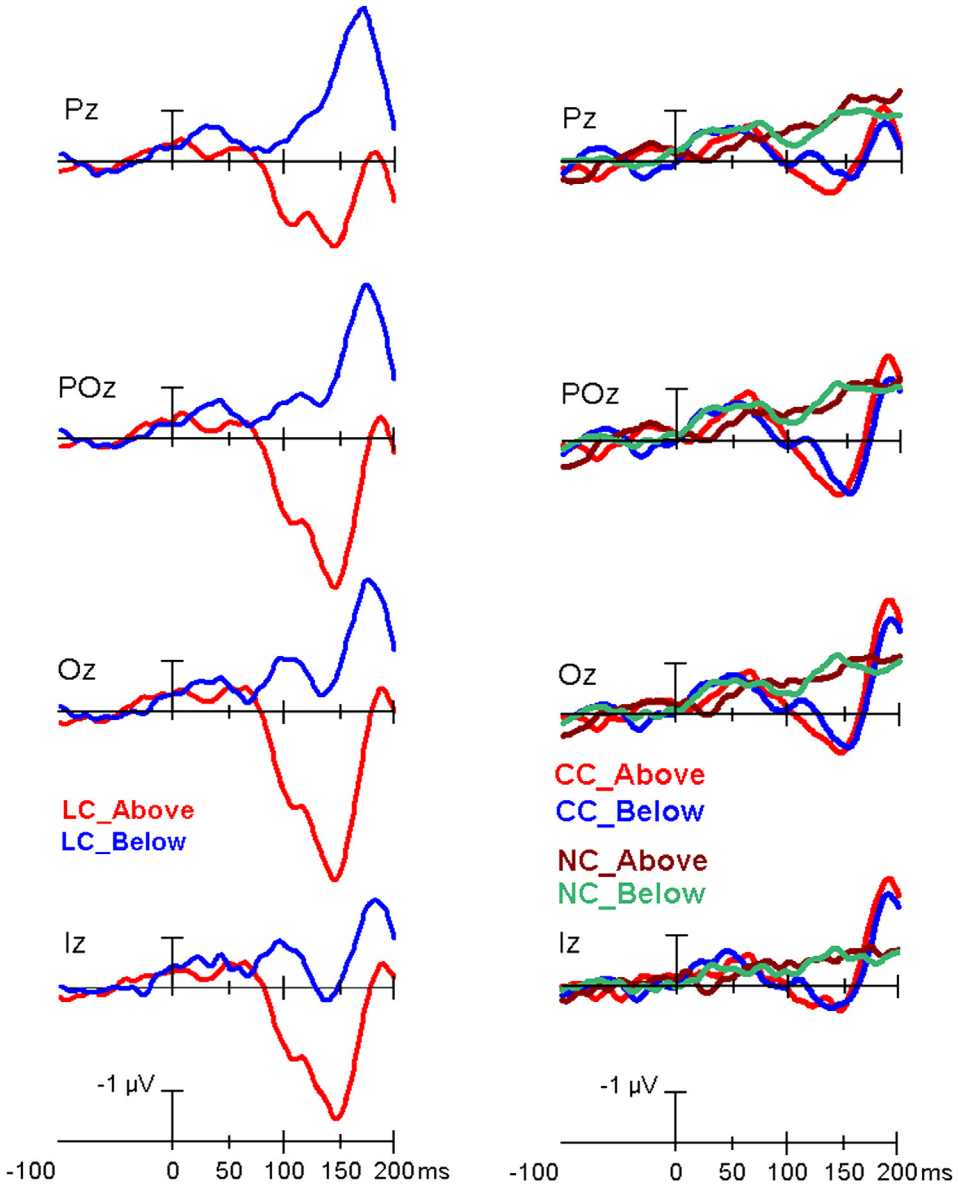

Figure 3. Left: grand-average ERPs recorded at midline parietal (Pz), parietal-occipital (POz), occipital (Oz), and inion (Iz) in response to trials with LC presented in the UVF as compared with grand-average ERPs elicited by those trials with LC falling in the LVF. **Right:** grand-average ERPs recorded at the same midline electrodes in response to trials relative to CC and NC conditions as a function of following target-related UVF and LVF. Note that ERP waveforms have been plotted with a blown-up time scale going from -100 ms before presentation of the different cue conditions until 200 ms after their delivery or omission to highlight the earliest occipital activations.

occipital (POz), occipital (Oz), and inion (Iz) midline sites (see Figure 3 for ERPs obtained at these sites) as well as mesial–occipital (O1 and O2) and mesial- and lateral parietal–occipital (PO3 and PO4) electrodes (see Figure 4 for ERP waveforms recorded at these sites). Mean amplitude values of C1 and C2 were statistically analyzed for any significant difference by means of separate multifactorial repeated–measures ANOVAs carried out by means of STATISTICA 7.0.

2.6.1. Midline electrodes

One set of three-way ANOVAs (one for each time window: C1, C2) was carried out on data recorded at midline sites. Relative factors included: cuing type (3 levels: CC, LC and NC), target-related location ("location"; 2 levels: UVF or LVF), and electrode (4 levels; Pz, POz, Oz, Iz).

2.6.2. Lateral electrodes

Another set of four-way ANOVAs (one for each time window: C1, C2) was carried out on data recorded at lateral electrode sites. Relative factors included: cuing type (3 levels: CC, LC and NC), target-related location ("location"; 2 levels: UVF or LVF), electrode (2 levels: O1, O2, PO3, PO4), hemisphere (Hem; 2 levels: left vs. right).

Besides the repeated-measures ANOVA effects we reported generalized effect sizes [59, 60], η^2_g, for these analyses. The Greenhouse-Geisser correction was also applied to compensate for possible violations of the sphericity assumption associated with factors which had more than two levels. In this case, the degrees of freedom accordingly modified are reported together with the epsilon (ε) and the corrected probability level. Post hoc Tukey tests were used to compare the difference between means for significant main and interactional factors with more than 2 levels only. Statistical significance was considered which started at $p < 0.05$ and expectantly reached lower levels. The contrasts reflecting the functional activation or deactivation of neural networks separately regulating alertness (CC vs. NC) and spatial attention orienting (LC vs CC) are reported in Table 1.

2.7. ERPs intracranial source reconstruction methods

To tap at brain intracranial origins of attentional effects as mirrored by ERPs at the scalp, separate source reconstructions were carried out on LC – CC ERP difference waves (DWs) grand-averaged over the participants' sample, within the two diverse cue-related time spans of P-N80. This was done separately for UVF and LVF target locations using an improved version of *Low Resolution Electromagnetic Tomography* (LORETA [61]), namely the standardized Low Resolution Electromagnetic Tomography (i. e., sLORETA [62]), which incorporates a singular value decomposition-based lead field weightings. sLORETA computes an activation probability, which is the fraction of times where the simulated dipole position is active with a value greater than the 60% of the maximum current source density (CSD) distribution, divided by the total number of realizations. The location of the regions of interest is determined by looking where the CSD lies above this specific threshold. The statistical probability of source activation based on Fisher's F-test is provided for each independent dipole or EEG source, whose import is reported as the dipole magnitude value. These probability solutions have been shown to be highly robust when based on group data rather than on single individual findings [63, 64]. sLORETA is complemented by equivalent dipole modelling. The electromagnetic dipoles are shown as arrows and indicate the position, orientation and magnitude of the dipole modelling solution applied to the ERP difference wave in the specific time window.

To perform sLORETA, a standard realistically shaped *boundary element model* (BEM), stored in the Master PC, was used. The BEM consisted of a set of T1-weighted 3D MRI brain images, implemented in the ASALab package, and was based on one homogenic compartment made up of a lead field matrix of 1389 weighted values [65]. The same default sets of electrode labels and 3D locations as those used during EEG recording were imported from the Master PC hard disk. The combination of these default sets of EEG channel denominations and locations as well as of brain images was then used for source reconstruction in both the C1 and C2 time intervals of the LC-CC difference waves of the grand-average ERPs.

Before computations, sLORETA automatically re-referenced scalp-recorded ERPs to average-channels. Source space properties was based on a grid spacing of 15 mm, while the Tikhonov regularization value derived from an estimated SNR = 3. Dipole coordinates computed by ASALab-based sLORETA were then used to obtain both human brain structures and Brodmann area (BA) labels, as available in the Talairach and Tournoux [66] atlas, by means of the gray-matter search range option of the version 2.4.3 of the Talairach Client or Talairach Daemon, the renowned high-speed Web Database created and developed by Jack Lancaster, Peter Fox and colleagues [67, 68].

2.8. Behavioral data recording and analysis

Behavioral data (motor response speed (RTs), errors and omissions) were analyzed to measure whether spatial attentional cueing was effective in manipulating attention deployment in comparison to both the simply alerting and the lack of any pre-cueing conditions. Also, we investigated whether the target anisotropic position significantly affected

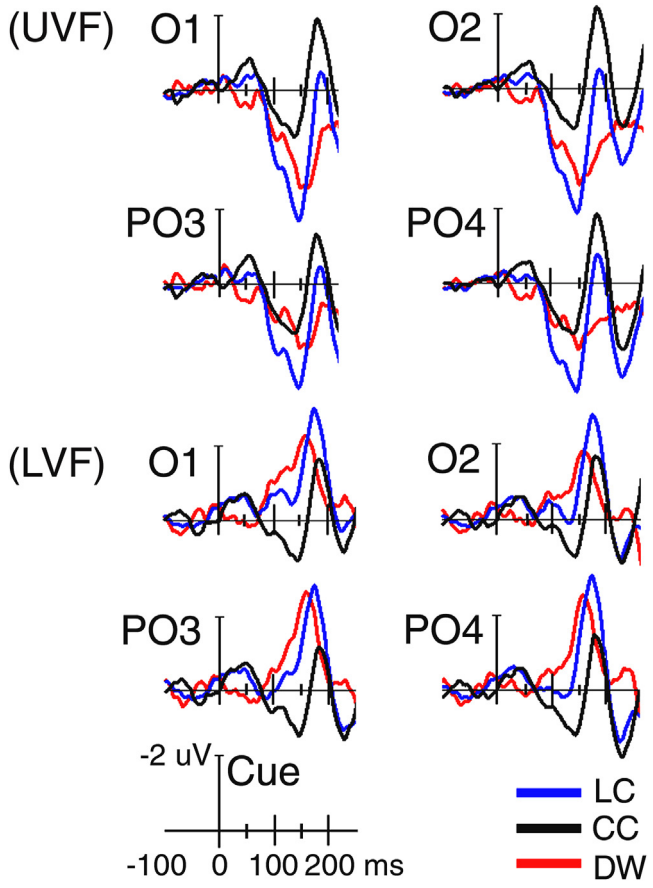

Figure 4. UVF: grand-average ERPs recorded at homologous mesial-occipital (O1-O2) and mesial parietal-occipital (PO3-PO4) sites elicited by a spatial cue (LC) validly preceding targets falling in the upper UVF as compared with grand-averaged ERPs elicited by a central cue (CC) presented prior targets falling in the same field. The difference wave (DW) has also been plotted as computed subtracting ERPs to CC from ERP to LC. **LVF:** same as for UVF, except that here LC and CC preceded targets falling in the LVF. Note that for all conditions, ERP waveforms have been plotted with a blown-up time scale going from -100 ms before cue presentation until 250 ms after its delivery to highlight the earliest morphological differences found in the waveforms across the two visual fields.

Table 1. Statistical significances (p values) obtained from ANOVA post-hoc comparisons for alertness and for attention orienting modulations reported separately for the C1 and C2 time-spans of the P/N80 sensory response, as well as for the midline and lateralized electrodes. It was expected that attentional effects increased as time progressed (going from C1 to C2), that Attentional allocation (LC vs. CC contrast) affected the earliest response especially at mesial occipital sites (Oz, but also O1 and O2) and that Alertness (CC vs. NC contrast) affected the earliest response at more lateral sites (e.g. POz, or PO3 and PO4). The "tilde" character, ~, indicates a trend toward the reported direction. UVF = Upper Visual Field; LVF = Lower Visual Field; POS = Positive; NEG = Negative. n.s. = not significant. LH = Left hemisphere; RH = Right hemisphere; Tgt. Location = Target-related location.

TIME RANGE	MIDLINE ELECTRODES				POLARITY
	PZ	POz	Oz	Iz	Polarity
C1 (60–75 ms)					
Upper Visual Field					
Alertness CC vs NC	n.s.	n.s.	n.s.	n.s.	~POS
Attention LC vs CC	0.05	0.01	0.001	n.s.	POS
Lower Visual Field					
Alertness CC vs NC	0.01	0.01	n.s.	n.s.	~POS
Attention LC vs CC	0.05	0.01	0.05	n.s.	POS
Upper	n. s.	n. s.	0.04	n. s.	NEG
Lower	n. s.	n. s.	0.04	n. s.	POS
C2 (75–90 ms)					
Upper Visual Field					
Alertness CC vs NC	n.s.	n.s.	0.004	n.s.	POS
Attention LC vs CC	0.048	0.00001	0. 01	~0.09	POS
Lower Visual Field					
Alertness CC vs NC	n.s.	0.01	0.04	~0.06	POS
Attention LC vs CC	n.s.	0.04	0.01	0.001	NEG

TIME RANGE	LATERAL ELECTRODES		POLARITY
C1 (60–75 ms)	**O1-O2**	**PO3-PO4**	POS
Upper	0.01	n.s.	NEG
Lower	0.01	n.s.	POS
Alertness CC vs NC	LH: 0.0001 RH: 0.0001	LH: 0.0001 RH: 0.0001	POS
Attention LC vs CC	LH: 0.001 RH: 0.001	LH: 0.001 RH: n.s.	POS
C2 (75–90 ms)			
Upper Visual Field			
Alertness CC vs NC	n. s.	n. s.	~POS
Attention LC vs CC	0.001	0.001	POS
Lower Visual Field			
Alertness CC vs NC	0.001	0.0001	POS
Attention LC vs CC	n. s.	n. s.	~NEG
Upper Visual Field			
Alertness CC vs NC	LH: n. s. RH: n. s.	LH: n. s. RH: n. s.	~POS
Attention LC vs CC	LH: 0.0001 RH: 0.0001	LH: 0.0001 RH: 0.0001	POS
Lower Visual Field			
Alertness CC vs NC	LH: n. s. RH: 0.0001	LH: 0.0001 RH: 0.0001	POS
Attention LC vs CC	LH: 0.0001 RH: 0.0001	LH: 0.0001 RH: 0.0001	POS

the speed and efficiency of behavioral motor responses. A two-way repeated-measures ANOVA with cueing type (CT = 3 levels; CC, LC and NC) and target-related location (2 levels; UVF and LVF) as experimental factors was carried out on the RTs. Error percentages were analyzed by means of a repeated measures ANOVA with the same experimental design as for the RTs. A count of response omissions showed that the volunteers committed very few of these faults. A repeated-measures ANOVA with the same design as for the error and RTs was carried out on these data. Before being submitted to the multifactorial repeated-measures ANOVA, error rate percentages were transformed in ϕ (*arcsine*) degrees because percentage values do not exhibit homoscedasticity [69], which is necessary for ANOVA. In fact, the distribution of percentages is binomial, whereas the arcsine transformation of the data makes the distribution normal [70].

The data for this experiment are available for reference, upon specific request of peer scientists.

3. Results

3.1. Results of behavioral performance speed and efficiency analyses

Behavioral analyses were performed on a sample of 21 participants. Indeed, the EEG data of 4 of them were rejected due to technical problems.

3.1.1. Reaction times

Among other significant effects of the main factors, the ANOVA highlighted the two-ways interaction of cueing condition x target-related location ($F(2; 40) = 7.2$; $p < 0.002$; $\varepsilon = 1$). Tukey post-hoc contrasts for the two-ways interaction indicated that, no matter target location considered, LC induced faster RTs than both CC and NC, while, in turn, CC produced faster RTs than NC, as can be clearly appreciated in Figure 5. Further post-hoc contrasts also indicated that, unlike for CC and NC conditions, for LC RTs were significantly faster when targets were delivered in the UVF than in the LVF ($p < 0.0001$).

3.1.2. Error percentages

A significant main effect of target-related location ($F(1; 18) = 12.24$; $p < 0.001$; $\varepsilon = 1$) showed a smaller errors rate for the UVF ($M = 1.44$; S.E. $= 0.3$) than for the LVF ($M = 2.05$; S.E. $= 0.4$). However, Tukey post-hoc comparisons for a significant interaction of cueing type x target-related location ($F(2,36) = 5.46$; $p < 0.0001$; $\varepsilon = 0.824$) revealed that the aforesaid effect depended on a significant larger error rate for the LVF than for the UVF only when the targets were preceded by a CC ($p < 0.0001$). Further post-hoc comparisons also showed that, unlike for the UVF, for the LVF the errors rate for the CC condition was robustly higher than for the NC condition ($p < 0.001$), but not for the LC one, for which only a trend was observed.

3.1.3. Omissions

The repeated-measures ANOVA did not yield any significant differences in missed response rates across experimental factors.

3.2. Electrophysiological results

3.3. P-N80 mean amplitude measured at midline electrodes

3.3.1. 60–75 ms time span (C1). The ANOVA showed that C1 mean amplitude significantly varied as a function of the interaction of target-related location x electrode ($F(2.13; 34.04) = 4.47$; $p < 0.0171$; $\varepsilon = 0.71$; $\eta^2_g = 0.22$). Indeed, no matter the cuing mode, a greater negativity was elicited by a cue when the target appeared in the UVF than in the LVF at Oz site (see Table 1 for statistical post-hoc significance values). However, the interaction of target-related location x cuing x electrode ($F(3.69; 53.88) = 2.62$; $p < 0.048$; $\varepsilon = 0.72$; $\eta^2 = 0.18$) and relative post-hoc comparisons also showed that C1 was significantly more negative for the UVF than the LVF ($p < 0.041$) at Oz site for the LC condition only (See Figure 6 for mean and S.E. values). Single comparisons also proved that, no matter the target-related location considered, LC elicited a more positive C1 than CC at all midline electrodes, except at the Inion (i. e., Iz). Conversely, alerting – as obtained by means of the CC Vs. NC contrast – significantly affected C1 amplitude at Pz and POz electrode sites only, exclusively when preceding the target arrays flashed in the LVF (see Table 1 again and Figure 6 again for these findings).

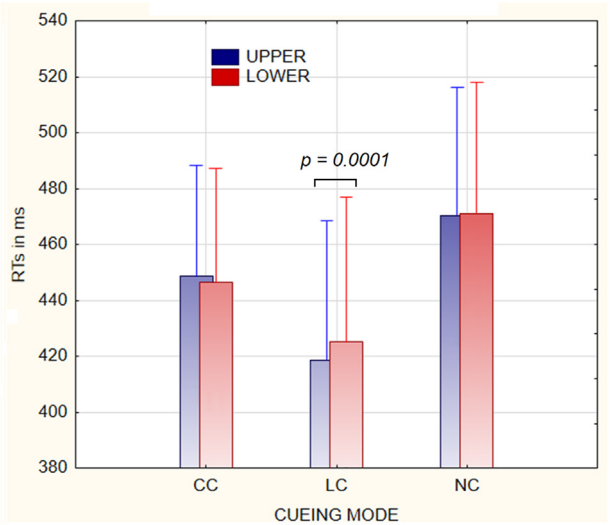

Figure 5. RT mean and S.E. values as a function of the two-ways interaction of cueing type x Target-related condition. Worth of note is that for LC, unlike for CC and NC, RTs to the UVF targets were faster than the RTs to the LVF targets.

3.3.2. 75–90 ms time span (C2). The significant interaction of cuing type x target-related location x electrode Tgt. Location x Cueing type x Electrode ($F(4.38; 56.22) = 2.42$; $p < 0.048$; $\varepsilon = 0.69$; $\eta^2 = 0.15$) and relative post-hoc contrasts showed a significant effect of the local cuing of spatial attention (i. e., LC vs. CC) at all sites, except at Iz. Additionally, a significant alerting effect (i. e., CC vs. NC) was shown at Oz electrode only (see Table 1 for *p* values and Figure 7 for mean and S.E. values). Both attention orienting and alerting effects were reflected by cuing-related increases in C2 positivity (see the polarity of attention effects in Table 1).

As for the LVF, tests for simple effects showed a significant influence of attentional orienting (i. e., LC vs. CC) at POz, Oz, and Iz sites, which, unlike for C1, manifested as an enhanced negativity (see again Table 1 and Figure 7 for these findings.) Additional assessments also laid it out a significant alerting modulation (i. e., CC vs. NC), consisting in an enhanced positivity at POz and Oz sites (see Table 1 again and Figure 7).

3.4. P-N80 mean amplitude measured at lateral electrodes

3.4.1. 60–75 ms time span (C1)

The ANOVA carried out on C1 mean amplitude yielded a significant interaction of target-related location x electrode ($F(1,16) = 4.27$; $p < 0.05$; $\varepsilon = 1$; $\eta^2 = 0.210$). C1 was more negative for the UVF ($M = -0.34$ μV, S. E. $= 0.12$) than the LVF ($M = -0.18$ μV, S. E. $= 0.14$) at O1-O2 mesial-occipital sites only (see Table 1 for the post-hoc statistical significances). Cuing type main factor was also found to be significant. Post-hoc contrasts indicated that C1 was more positive to LC ($M = 0.016$ μV, $SE = 0.18$) than to NC ($M = -0.54$ μV, $SE = 0.16$), but not than to CC ($M = -0.23$ μV, $SE = 0.13$). Most importantly, at this earliest latency, cuing type significantly interacted with both hemisphere and electrode factors ($F(1.67; 26.80) = 4.33$; $p < 0.029$; $\varepsilon = 0.92$; $\eta^2 = 0.213$). Post-hoc comparisons revealed that this modulation consisted in a greater positivity measured at the mesial-occipital sites over both hemispheres, but

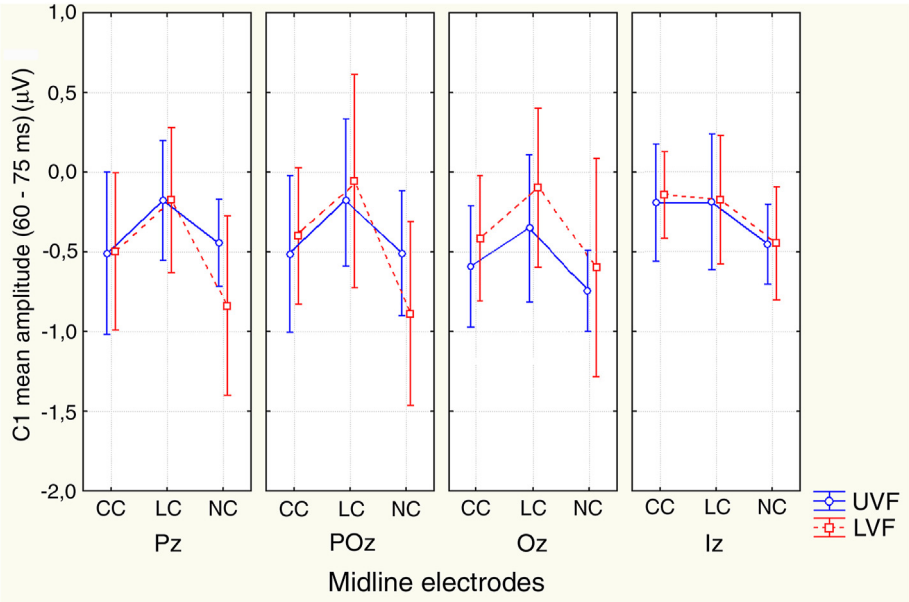

Figure 6. C1 mean amplitude and 95% confidence interval values measured in between 60 – 75 ms at the midline posterior electrodes as a function of CC, LC, and NC cuing mode as well as of the target-related UVF and LVF. Most interestingly, no matter the target-related visual field considered, LC elicited a greater positivity than CC at all electrodes, except at the Inion. These results suggest the occurrence of an earliest positive attentional priming of posterior scalp sites voltage.

only at the left-sided lateral parietal-occipital site, for orienting of attention (i.e., LC vs. CC), no matter the target- location (see Figure 4 and Table 1). Simple comparisons also made clear that alerting (i. e., CC vs. NC) elicited a higher positivity at both the mesial- and lateral-parietal-occipital leads of both hemispheres (see Table 1 again).

3.4.2. 75–90 ms time span (C2)

The triple interaction between cuing type, target location and electrode ($F(1.67; 26.81) = 5.17$; $p < 0.01$; $\varepsilon = 0.84$; $\eta^2 = 0.24$) and the quadruple interaction of cuing type x target location x hemisphere x electrode ($F(1.48; 23.27) = 3.41$; $p < 0.05$; $\varepsilon = 0.73$; $\eta^2 = 0.18$) were also significant. Post hoc analyses for this 4-way interaction proved that for LC attention orienting enhanced positivity was measured at both the mesial–occipital and parieto-lateral occipital sites of both hemispheres for the UVF, but not for the LVF (Figure 4, the maps of Figure 2, and Table 1). Conversely, for alerting condition a significant larger positivity was obtained at all electrodes over both hemispheres for the LVF, but not for the UVF, which did not show any significant differences (see Figure 4 and Table 1 again)

3.4.3. Source analyses and results

Inverse solutions were computed by means of sLORETA on the difference waveforms obtained subtracting grand-average ERPs to CC from those to LC. Separate computations were carried out for orienting of

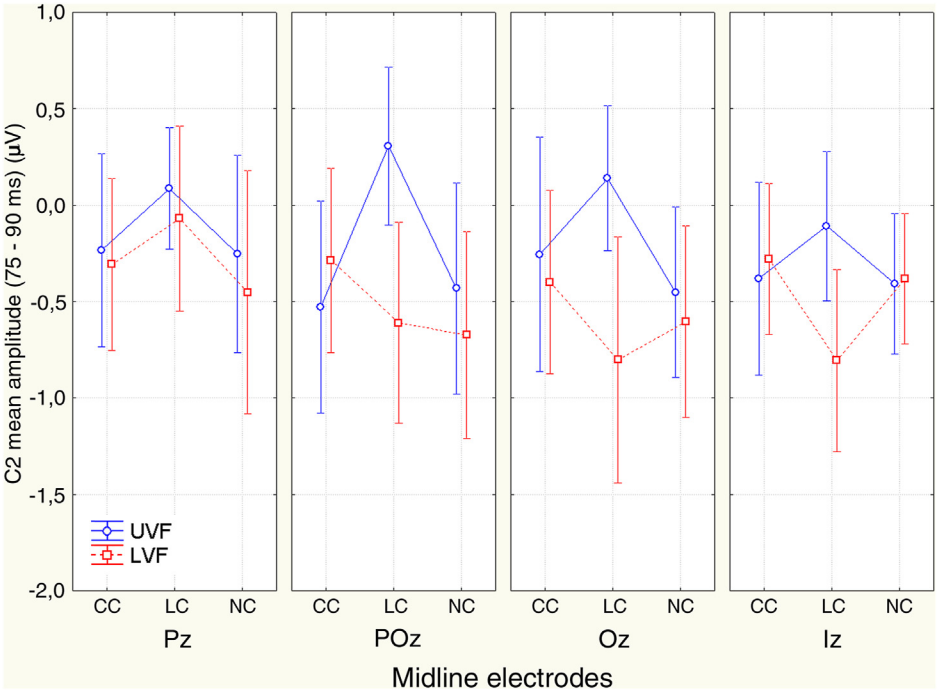

Figure 7. ERPs C2 mean amplitude and 95% confidence interval values measured in between 75 -90 ms at the midline posterior electrodes as a function of CC, LC and NC cuing mode as well as of the target-related locations. It is noteworthy that, except for the parietal site (Pz), at all other electrodes LC elicited a greater positivity than CC for the target-related UVF and a greater negativity for the target-related LVF, respectively. Overall, these findings suggest the occurrence of an earliest attentional priming of visual areas, recorded at the posterior scalp sites as opposite-polarity modulations as a function of the visual field considered.

spatial attention toward the UVF and LVF and for the two 60–75 ms and 75–90 ms time-spans. To highlight the activations of the early districts of the visual system, active equivalent dipoles or neural generators selectively localized in the occipital cortices are displayed overimposed on T1-weighted 3D MRI brain scans separately for the aforementioned conditions in Figures 8 and 9. The full lists of active dipoles and of their coordinates, as related to Brodmann areas (BA)-labeled human brain structures reported in the Talairach and Tournoux (1988) atlas, are provided in Table 2 and Table 2 for the 60–75 ms and 75–90 ms time-spans, respectively.

4. Discussion

In the present study, targets were randomly presented in the upper visual field (UVF) and lower visual field (LVF) along the vertical meridian while being preceded by different cuing conditions: namely, a valid spatial orienting cue (LC) signaling target location, a spatially neutral, alerting central cue (CC), and a no-cue (NC) condition. For comparison purposes across cuing conditions, behavioral and ERP responses were averaged as a function of the following target location for each of the reported cuing contingencies.

In line with previous literature, behavioral data indicated that, compared with lack of any pre-cueing (i.e., NC), a previous alerting (i.e., CC) or a prior orienting of visual attention to the point in space of a following target array (i.e., LC) induced a progressive improvement in performance levels. Indeed, RTs were the fastest for LC, of intermediate speed for CC and the slowest for NC condition (e. g., Fan *et al*, 2002) [56]. Going beyond these studies, however, our data also indicated that RTs were overall faster for the UVF than the LVF target-arrays. Accuracy data also indicated that, when targets were preceded by a CC, volunteers committed less errors when targets fell in the UVF than the LVF. In addition, unlike for the targets presented in the UVF, for which no differences were found between the percentages of error committed across cueing types, for the targets flashed in the LVF, the CC induced a larger number of errors than NC. It seems possible that this difficulty was very probably related to a less efficient disengagement and reorienting of spatial attention to targets falling in the LVF. Overall, then, our behavioral data indicated a vertically-oriented anisotropy in the speed and accuracy of attentional control between the UVF and LVF, showing a bias favoring the upper visual field. This support the hypothesis of an anisotropic asymmetry across the horizontal meridian between the visual fields for both visual perceptual and top-down attentional control processes [70, 71,72].

Although directly related to the early phases of attention orienting and alerting induced by different pre-cuing modes, our electrophysiological data suggested that this asymmetry in attentional capacity and control across the visual horizontal meridian already occurs at the earliest post-cueing processing latency ranges. Indeed, our ERP earliest responses to cues showed a significant polarity swapping as a function of target-related visual field stimulation across the horizontal meridian for LC at both midline-occipital (i. e., Oz) and mesial-lateral occipital (i. e., O1-O2) electrode sites (see maps of Figure 2 and ERPs of Figures 3 and 4). ERP data also indicated that the bioelectrical sign of this polarity swapping changed as a function of the visual field as neural processing progressed in time, starting from the initial occipital cortical response volley. Indeed, in the 60–75 ms time range, C1 component inverted in polarity as a function of cueing across the horizontal meridian, appearing as significantly more negative (i.e., less positive) in response to UVF cues and as significantly less negative (i.e., more positive) in response to LVF cues. It is interesting that these results fully agree with previous findings in the literature although the latter concern C1 response to targets [17, 18, 19, 20, 21, 22, 23, 24, 25, 26, 73]. Following this initial sensory volley, a clear-cut opposite polarity trend was found as a function of the cued visual field: namely, a strong positivity (C2) was found for the UVF and a negativity for the LVF. These findings are fully consistent with those of previous studies reporting an opposite trend for C1 response when stimulation across the horizontal meridian of the visual space falls along the vertical meridian of this space (i. e., positive for the UVF and negative for the LVF) is recorded [19, 20, 21, 22, 23, 27, 28]. In a recent study, Capilla *et al.* [29] defined this voltage trend, naming it C2 component. Based on source reconstruction procedures, these authors found that, unlike the C1, C2 reached its maximum amplitude along the vertical meridian and arose from the confluence of V1 and V2, where the vertical meridian would be mostly represented [28, 30, 31]. Then, it seems reasonable to think that the C2 is mostly generated in occipital cortex regions outside the calcarine fissure as V2, rather than V1, given that (i) the waveform and timing of this component closely parallels the one predicted for V2 [32]. This is in agreement with our source reconstruction findings showing both V1 (BA17) and V2 and V3 (BA 18/19) areas as being involved in the spatial attentional modulation, among several other areas, at these earliest visual post-cuing processing (see Figures 8 and 9 for dipolar anatomical sources and Tables 2 and 3 for their detailed lists).

Most importantly, as the C1 response is concerned, our findings seem to indicated that, no matter the visual field considered and the polarity

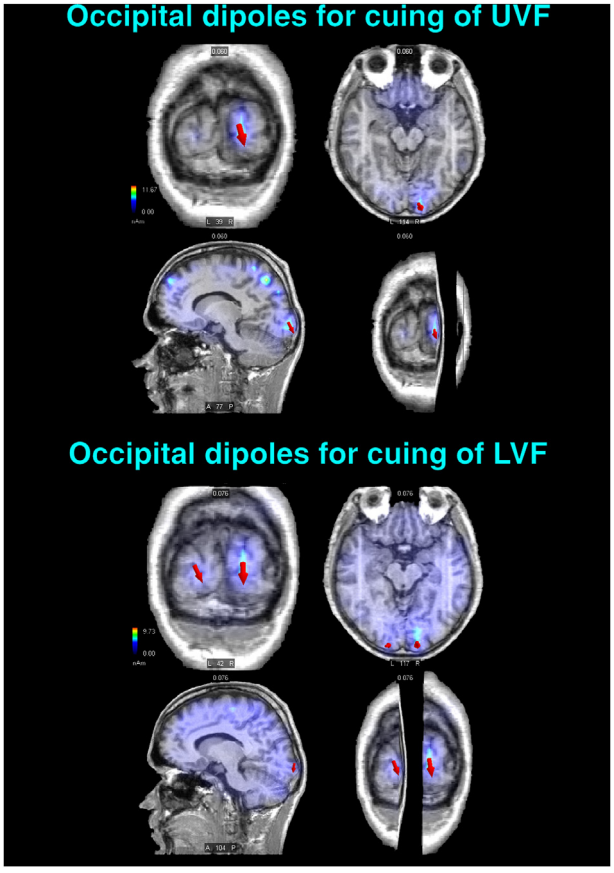

Figure 8. Selected striate-occipital sources of sLORETA inverse solutions computed in the C1 latency range (i. e., 60–75 ms) of the P-N80 complex for the LC - CC DW relative to the cuing of visuospatial attention toward either the UVF (Left) or the LVF (Right). The active equivalent dipoles overimposed on realistic (left-to-right) coronal, axial, parasagittal, and 3D T1-weighted MRI brain images are drawn as red arrows with different sizes according to their magnitudes and different orientations according to their flowing direction. **Upper Panel:** a prominent source of activation localized in the right-sided striate occipital portion of the lingual gyrus (LG, BA 17; ROI = 2 mm) is shown for the UVF. **Lower Panel**: equivalent dipoles reflecting active sources localized in the striate occipital portions of both the lingual and cuneus gyri (BA 17; ROI = 2 mm) of both hemispheres elicited by the cuing of LVF. Note that the complete list of all the active dipoles obtained by means of the sLORETA inverse solutions for C1 and detailed information about their features are reported in Table 2. L = Left; R = Right.

shown by this component across the horizontal meridian, LC elicited a significant greater positivity with respect to CC at the midline parietal, parietal-occipital and occipital electrodes, besides at mesial-occipital and parietal-occipital electrodes. In our view, these findings suggest that C1 voltage did not change simply as a function of the stimulation of the opposite retino-corticotopic banks induced by LC presentation (in the UVF or LVF) with respect to central point (as for CC). Rather, it seems probable that the increased positive voltage for this component might also reflect an attentional biasing of striate occipital areas activity, already starting at this earliest post-cue latency, for subserving the following selective processing of information falling at spatially relevant locations. This attentional enhancement of striate activity would result in an improved sensory representation of the stimuli falling within the focus of spatial attention. As a possible consequence, attention would improve performance by concentrating processing resources at the attentional focus through the modulation of striate neurons response as a function of their receptive fields. At this regard, evidence has been provided that early spatial attention modulation improves visual search, acuity, texture segmentation and spatial frequency perception [73, 74]. In our opinion

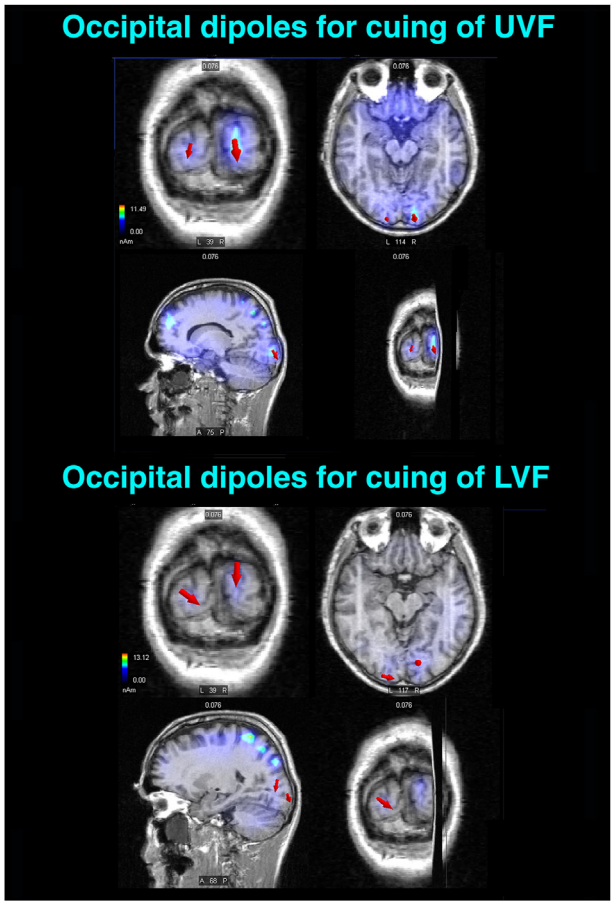

Figure 9. Same as for Figure 8, except that sLORETA inverse solutions were carried out on ERPs C2- latency range (i. e., 75–90 ms) of the P-N80 complex. **Upper Panel:** an active source is plotted (see red arrow) in the striate portion of the right-sided lingual gyrus (BA 17; ROI = 2 mm) of the occipital pole. Moreover, a smaller dipole generating from the striate portion (BA 17) of the lingual gyrus of the left hemisphere is drawn (see downward pointing arrow). **Lower Panel:** a large downward-going dipole localized in the striate cuneus (BA 17) of the right hemisphere, together with a rightward-going dipole localized in the striate-portion of the lingual gyrus of the left hemisphere (see red arrows) are mapped on brain images for the LVF. Note that the complete list of all the active dipoles obtained by means of the sLORETA inverse solutions for C2 and detailed information about their features are reported in Table 3. L = Left; R = Right.

that the findings of an increased voltage for the spatially orienting cueing condition might reflect an attentional biasing would be also supported by our source reconstruction data. Indeed, inverse solutions not only included active equivalent dipoles mapped to striate occipital cortices (e. g., lingual and/or cuneus gyrus, BA17; Table 2), but also to brain areas controlling orienting of spatial attention such as prefrontal areas (e. g., MFG, BA6 and/or MFG, BA8) as well as the upper parietal lobules (e. g., UPLs, BA7), at both visual fields (see Figure 8 and Table 2).

As for the retino-corticotopic attentional activation, the present findings agree with those reported by many studies in the literature: that is, a modulation of the earliest C1 to targets induced by orienting of spatial attention toward both visual receptive fields across the horizontal meridian [21, 22, 25, 36, 38]. However, they are inconsistent with the findings reported by some other studies using rather different experimental paradigms [39, 75], which found a significant C1 modulation for the upper, but not the lower visual field.

At this regard, it can be hypothesized that this inconsistency might be related to the different anatomo-physiological organization of the various portions of the cortical-retinal routes stimulated. Indeed, there are findings indicating that stimulation near or along the vertical meridian of the visual field within the earliest sensory processing range actively involves the activation of regions outside the calcarine fissure, such as, for instance, V2 and V3, besides of regions within it (i. e., V1). The latter activations would be reflected at the scalp surface by a reversed polarity C2, compared to that found for C1: namely, a positive-going C2 is recorded for UVF as opposed to a negative C2 for the LVF [28, 29].

This seems to be consistent with what found in the present study for the P-N80 complex. As well visible in the time series voltage maps of Figure 2, for an initial short time span of P-N80 (i. e., 60–75 ms), possibly reflecting the renown C1 early activation predominated by V1 activity [76], voltage topography at occipital-parietal sites is negative for the presentation of the LC in the superior UVF and positive for presentation of this same cue type in the LVF. Consistently, in this shortest C1-related lapse of time, orienting of spatial attention results at the scalp in a positive modulation, no matter the visual field cued (see voltage mapping for the Diff. waves of Figure 2). As the trend for this initial sensory volley of P-N80 is concerned, our findings are in full agreement with the proposal that only this earliest volley is truly reflecting the C1-eliciting (i. e. C1*early*) V1 activation. At this regard, it is interesting that the inverted solutions of source reconstructions carried out for C1 showed a robust asymmetric activation of the right-sided striate occipital cortices (i. e., lingual gyrus; BA17/cuneus gyrus; BA17; ROI: 2 or 3 mm, respectively) for the UVF, compared to the more distributed striate generators across hemispheres (i. e., bilateral lingual/cuneus gyri; BA17; ROI: 2 or 3 mm, respectively) for the cuing of the LVF (see Figure 8 for an illustration of this findings and Table 2 for a complete dipoles list).

Following the C1 sensory volley, in between 75-90 ms post-stimulation a clear-cut inversion in polarity can be appreciated in the maps for LC as a function of the visual field with respect to CC: namely, a strong positivity was elicited by cues flashed in the UVF and a negativity by cues in the LVF. These results are consistent with the C2-related trend reported in the literature, predominated by V2 and V3 activity [27, 29]. As a consequence, attentional modulation derived by the difference waves results in an increase in positivity focused at midline-occipital (Oz) and parietal-occipital (POz) electrode sites as well as surrounding scalp regions for the UVF. Conversely, a relatively strong negativity, focused over midline-occipital and lower Inion sites, is visible in the maps for LC stimulation of LVF as the C2-related voltage is concerned (see Figure 7 for mean amplitude data). Therefore, a strong attention-related negativity, spread all over the midline-occipital and lower Inion as well as the inferior occipital-parietal sites, reflected attention orienting toward the LVF at the scalp. In full support of the voltage reversal trends mentioned above, source analyses for C2 revealed superficial striate generators symmetrically localized in the lingual gyri of both brain hemispheres for the cuing of the UVF. Conversely, a deeper striate occipital generator localized in the right-sided cuneus and a superficial generator confined in

Table 2. List of active brain sources found by means of sLORETA explaining the difference voltage in between 60-75 ms post-cueing (i. e., C1 deflection of P-N80) between the central (CC) and the local spatial cueing conditions (LC). Different sub-tables report data related to the cueing of spatial attention toward the upper or lower visual fields, respectively. Besides being separated as a function of anterior and posterior brain locations, active sources are ranked as a function of their magnitudes. Different source locations are reported as a function of the region of interest (i. e., ROI). Note that no ROI is reported where source location or Brodmann area (i. e., BA) did not change within a cube range of 3 mm. The Tailarach's and Tournoux's 3D coordinates (T) and ROIs are indicated in mm.

Mag	T – x	T – y	T – z	Hem	Lobe	ROI	Gyrus/Area	BA
ATTENTIONAL CUING OF THE UPPER FIELD								
Anterior Brain								
11.667	-29	41	38	L	F		Sup F	8
10.120	0	-43	62	L	F		Med F	5
8.975	-29	12	55	L	F		Mid F	6
7.551	14	56	37	R	F		Sup F	9
6.254	-14	-14	59	L	F		Mid F	6
Posterior Brain								
10.557	29	-42	62	R	P	3 mm	Post-C	5
						3 mm	Sup P	7
8.135	14	-97	-5	R	O	2 mm	Ling	17
5.945	-29	-79	21	L	O	2 mm	MOG	19
4.810	-29	-83	-16	L	O		Fusiform	18/19
4.497	-58	6	-2	L	T		Sup T	21
3.076	57	-19	0	R	T		Sup T	22
Mag	T – x	T – y	T – z	Hem	Lobe	ROI	Gyrus/Area	BA
ATTENTIONAL CUING OF THE LOWER FIELD								
Anterior Brain								
9.730	43	-15	44	R	F		Pre-C	4
8.227	43	11	41	R	F		Mid F	8
5.623	-29	41	38	L	F		Sup F	8
5.515	0	-27	60	L	F		Med F	6
5.034	14	56	37	R	F		Sup F	9
4.185	-29	12	56	L	F		Mid F	6
Posterior Brain								
6.840	29	-77	35	R	O	3 mm	Cun	19/7
6.534	14	-97	-5	R	O	2 mm	Ling	17
5.338	-14	-97	-5	L	O	2 mm	Ling	17
						3 mm	Cun	18
3.855	-43	-44	47	L	P		Inf P	40
3.747	-58	-32	17	L	T		Sup T	42
3.641	-43	-63	20	L	T		Mid T	21
3.457	-58	6	-2	L	T		Sup T	22
3.428	58	-20	-10	R	T		Mid T	21

Grid = 15 mm; Tikhonov correction SNR = 3. Cun = Cuneus; Hem = Hemisphere: L = Left; R = Right; F = Frontal; Fus = Fusiform; Inf = Inferior; Lb = Lobule; Ling = Lingual; Mag = Magnitude; Med = Medial; Mid = Middle; O = Occipital; MOG = Middle occipital gyrus; P = Parietal; Post = Posterior; PreC = Precentral; Sup = Superior. - = Intermediate.

the left-sided lingual gyrus was found for the cuing of the LVF (see Figure 9 for these findings and Table 3 for a complete list of the active dipoles). In the light of the more pronounced polarity-reversal, while sensory processing advances through the two processing substages of P-N80 complex for the LVF, it seems reasonable to hypothesize that this variability may possibly abate ERPs reflection of LVF attentional modulation when measurements span over the whole evoked potential and do not limit to the earliest C1 sensory volley.

It is challenging to compare our findings of earliest-latency effects involving striate occipital sources in response to cues directing visuospatial attention in space with those obtained by some dated electrophysiological studies cited above [50, 51, 52, 53]. This, not only because of the differences in the tasks used and of the slightly delayed timing of cue-related attentional modulation reported, but also because all these studies did not provide any information on ERPs intracranial sources. It is also intricate to compare our results with those reported by Woldorff et al. (2004) [54] and by Grent-t-Jong and Woldorff [55] despite their combining of ERPs and fMRI techniques, due to the different tasks used in these investigations. Conversely, a consistent general trend seems to exist between the findings of the present study and those reported by Hopfinger et al. [14], despite the different experimental methods based on ERPs recording and source computations of the former, with respect to the latter, based on fMRI indices. Nevertheless, two rather recent ERP studies failed to find significant signs of an earliest C1-attentional modulation (i.e., Baumgartner et al., 2018 [77]; Alilovic et al., 2019 [78]). We must outline that it is also hard to compare the lack of C1 effects reported in these studies with our data due to the many differences in tasks and EEG data analysis methodological solutions adopted. Indeed, our task was based on the randomized presentation of arrow target strings at two vertically opposite locations along the vertical meridian as preceded by different cue modes. Conversely, both the quoted studies used slightly, but differently modified versions of Kelly's et al. (2008) [21] original stimulus presentation task, based on the administration of stimuli at a variable set of lateralized locations around fixation to determine two diagonally opposite locations at which stimuli elicited a robust C1 for a given individual in a probe task, besides on a

Table 3. List of active brain sources found by means of sLORETA explaining the difference voltage recorded between 75-90 ms post-cueing (i. e., C2 deflection of P-N80) between the central (CC) and the local spatial cueing conditions (LC). Different sub-tables report data related to the cueing of spatial attention toward the upper or lower visual fields, respectively.

Mag	T – x	T – y	T – z	Hem	Lobe	ROI	Gyrus/Area	BA
ATTENTIONAL CUING OF THE UPPER FIELD								
Anterior Brain								
11.491	29	55	22	R	F		Sup F	10
10.004	-29	41	38	L	F		Sup F	5
7.602	-29	12	55	L	F		Mid F	6
6.344	-14	-14	59	R	F		Mid F	6
4.906	29	-14	59	R	F		Pre-C	6
3.527	43	11	41	R	F		Mid F	8
Posterior Brain								
9.756	29	-43	61	R	P		Sup P	7
8.862	14	-97	-5	R	O	2 mm	Ling	17
5.943	-29	-79	21	L	O	2 mm	MOG	19
5.867	- 14	-97	-5	L	O	2 mm	Ling/Cun	17/18
3.503	57	-50	-8	R	T		Mid T	37
2.094	57	-19	0	R	T		Sup T	21
Mag	T – x	T – y	T – z	Hem	Lobe	ROI	Gyrus/Area	BA
ATTENTIONAL CUING OF THE LOWER FIELD								
Anterior Brain								
9.730	43	-15	44	R	F		Pre-C	4
8.227	43	11	41	R	F		Mid F	8
5.623	-29	41	38	L	F		Sup F	8
5.515	0	-27	60	L	F		Med F	6
5.034	14	56	37	R	F		Sup F	9
4.185	-29	12	56	L	F		Mid F	6
Posterior Brain								
13.118	29	-42	62	R	P	3 mm	Post-C	
Sup P	5/7							
6.033	14	-80	7	R	O	2 mm	Cun	17
						3 mm	Ling	18
6.009	-14	-97	-5	L	O	2 mm	Ling	17
						3 mm	Cun	18
3.663	-58	6	-2	R	T		Sup T	22

validly-invalidly cued lateralized stimulus presentation spatial attentional task. To this must be added that, at least for Alilovic et al. (2019) [78], the influence of a further task load exerted by participants' stimulus prediction must also be considered. If Baumgartner et al. (2018) [77], comparing C1 to relevant vs irrelevant stimuli falling at validly and invalidly precued locations, failed to find early C1 effects, another study, using a relevant vs irrelevant spatial frequencies selection task (at both relevant vs irrelevant locations), found an object-based, space-selective C1 attentional modulation in between 40-60 ms post-stimulus (Proverbio et al., 2010) [23]. This evidence added to further previous and later C1 object-based attention modulation evidence provided by this same and other research groups as reviewed critically in Zani and Proverbio (2018) [79].

In conclusion, our findings seem to suggest a modulation of both C1 and C2 sub-components characterizing the P-N80 complex recorded in response to spatial attention cues. Despite the reverted inversion in polarity shown by these sub-components, an attention modulation was found for both the upper and lower fields of the visual space. Source analyses suggested that these modulations affected the activation of V1, besides of the higher-level V2 and V3 occipital cortices, respectively, especially for the LVF. In line with our ANT-based task, these attention-orienting effects might be related to the stimulation along the vertical meridian of the visual field, which has been proposed to be mostly represented by the V2 and V3 regions outside the calcarine fissure. Interestingly, notwithstanding the time span which separated the ERPs elicited by the cues and the behavioral motor response to targets, behavioral data showed consistent trends as the attention orienting and the visual field of stimulation were concerned. Indeed, RTs were faster for the attention orienting condition than for the alerting one, and for the UVF than for the LVF, respectively. Finally yet importantly, our data also lent support to the most recent views of visual attention postulating that neural selectivity is active at multiple levels within the visual system, indicating that, among these levels, a cuing-related earliest preparatory biasing of the striate and besides extrastriate cortices, may be included. Certainly, further investigation is needed to support and refine our account of selective spatial information processing and its retino-cortical underpinnings.

4.1. Study limitations

A potential limitation of our study is the relatively small sample size. Although 17 participants are enough for EEG studies, and many authoritative papers report an even smaller size, future studies should deal with this problem. The sample size was established based on previous literature and current psychophysiological guidelines (e.g., Faul et al., 2007) [80]. Furthermore, to control for possible alpha inflation due to multiple ANOVA comparisons, the Greenhouse–Geisser epsilon correction was applied. Notwithstanding that, the empirical results reported herein should be considered in the light of some limitations, which should be solved by replicating the study in larger populations.

One further limit, for some authors might be the *arcsine* transformation of behavioral data that tend to reduce numerical differences, being therefore a conservative method.

Declarations

Author contribution statement

Alberto Zani: Conceived and designed the experiments; Performed the experiments; Analyzed and interpreted the data; Wrote the paper.

Alice Mado Proverbio: Performed the experiments; Contributed reagents, materials, analysis tools or data; Wrote the paper.

Funding statement

Alberto Zani was supported by (National Research Council) CNR mainstream grants.

Data availability statement

Data will be made available on request.

Declaration of interests statement

The authors declare no conflict of interest.

Additional information

No additional information is available for this paper.

References

[1] N. Kanwisher, E. Wojciulik, Visual attention: insights from brain imaging, Nat. Rev. Neurosci. 1 (2000) 91–100.
[2] S. Kastner, M.A. Pinsk, Visual attention as a multilevel selection process, Cognit. Affect Behav. Neurosci. 4 (4) (2004) 483–500.
[3] M.S. Gazzaniga, R.B. Ivry, G.R. Mangun, Cognitive Neuroscience. The Biology of the Mind, fourth ed., W W Norton, New York, London, 2014, pp. 272–324. Chapter 7.
[4] D.A. Hayward, J. Ristic, Measuring attention using the Posner cuing paradigm: the role of across and within trial target probabilities, Front. Hum. Neurosci. 7 (205) (2013), https://doi.org/10.3389/fnhum.2013.00205.
[5] S. Kastner, P. De Weerd, R. Desimone, L.G. Ungerleider, Mechanisms of directed attention in the human extrastriate cortex as revealed by functional MRI, Science 282 (1998) 108–111.
[6] R.B. Tootell, N. Hadjikhani, E.K. Hall, S. Marrett, W. Vanduffel, J.t. Vaughan, A.M. Dale, The retinotopy of visual spatial attention, Neuron 21 (8) (1998) 1409–1422.
[7] J.A. Brefczynski, E.A. DeYoe, A physiological correlate of the 'spotlight' of visual attention, Nat. Neurosci. 2 (1999) 370–374.
[8] S. Kastner, M.A. Pinsk, P. De Weerd, R. Desimone, L.G. Ungerleider, Increased activity in human visual cortex during directed attention in the absence of visual stimulation, Neuron 22 (1999) 751–761.
[9] D. La Berge, M.S. Buchsbaum, Positron emission tomographic measurements of pulvinar activity during an attention task, J. Neurosci. 10 (1990) 613–619.
[10] D.H. O'Connor, M.M. Fukui, M.A. Pinsk, S. Kastner, Attention modulates responses in the human lateral geniculate nucleus, Nat. Neurosci. 5 (11) (2002) 1203–1209.
[11] S. Kastner, K. Schneider, K. Wunderlich, Beyond a relay nucleus: neuroimaging views on the human LGN, Prog. Brain Res. 155 (2006) 125–143.
[12] M.A. Silver, D. Ress, D. Heeger, Neural correlates of sustained spatial attention in human early visual cortex, J. Neurophysiol. 97 (2007) 229–237.
[13] M. Corbetta, J.M. Kincade, J.M. Ollinger, M.P. McAvoy, G.L. Shulman, Voluntary orienting is dissociated from target detection in human posterior parietal cortex, Nat. Neurosci. 3 (2000) 292–297.
[14] J.B. Hopfinger, M.H. Buonocore, G.R. Mangun, The neural mechanisms of top-down attentional control, Nat. Neurosci. 3 (2000) 284–291.
[15] G.R. Mangun, Neural mechanisms of attention, in: A. Zani, A.M. Proverbio (Eds.), The Cognitive Electrophysiology of Mind and Brain, Academic Press, London – New York, 2003, pp. 247–258.
[16] H.J. Heinze, G.R. Mangun, W. Burcher, H. Hinrichs, M. Scholz, T.E. Muente, A. Goes, M. Scherg, S. Johannes, H. Hundeshagen, M.S. Gazzaniga, S.A. Hillyard, Combined spatial and temporal imaging of brain activity during visual selective attention in humans, Nature (London) 372 (1994) 543–546.
[17] A. Martínez, L. Anllo-Vento, M.I. Sereno, L.R. Frank, R.B. Buxton, D.J. Dubowitz, E.C. Wong, H. Hinrichs, H.J. Heinze, H. Sa, Involvement of striate and extrastriate visual cortical areas in spatial attention, Nat. Neurosci. 2 (1999) 364–369.
[18] D.A. Jeffreys, J.G. Axford, Source locations of pattern-specific components of human visual evoked potentials. I. component of striate cortical origin, Exp. Brain Res. 16 (1972) 1–21.
[19] V.P. Clark, S.A. Hillyard, Spatial selective attention affects early extrastriate but not striate components of the visual evoked potentials, J. Cognit. Neurosci. 8 (1996) 387–402.
[20] A. Martínez, F. Di Russo, L. Anllo-Vento, M.I. Sereno, R.B. Buxton, S.A. Hillyard, Putting spatial attention on the map: timing and localization of stimulus selection processes in striate and extrastriate visual areas, Vis. Res. 41 (2001) 1537–1547.
[21] S.P. Kelly, M. Gomez-Ramirez, J.J. Foxe, Spatial attention modulates initial afferent activity in human primary visual cortex, Cerebr. Cortex 18 (2008) 2629–2636.
[22] S.P. Kelly, M.I. Vanegas, C.E. Schroeder, E.C. Lalor, The cruciform model of striate generation of the early VEP reillustrated, not revoked: a reply to Ales et al (2013), Neuroimage 85 (2013) 154–159.
[23] A.M. Proverbio, M. Del Zotto, A. Zani, Electrical neuroimaging evidence that spatial frequency-based selective attention affects V1 activity as early as 40-60 ms in humans, BMC Neurosci. 6 (11) (2010) 59.
[24] A. Zani, A.M. Proverbio, Attention modulation of short latency ERPs by selective attention to conjunction of spatial frequency and location, J. Psychophysiol. 11 (1997) 21–32.
[25] A. Zani, A.M. Proverbio, Selective attention to spatial frequency gratings affects visual processing as early as 60 msec poststimulus, Percept. Mot. Skills 109 (1) (2009) 140–158.
[26] J.V. Odom, M. Bach, M. Brigell, G.E. Holder, D.L. McCulloch, A.P.T. Vaegan, ISCEV standard for clinical visual evoked potentials (2009 update), Doc. Ophthalmol. 120 (1) (2010) 111–119.
[27] F. Di Russo, A. Martinez, M.I. Sereno, S. Pitzalis, S.A. Hillyard, Cortical sources of the early components of the visual evoked potential, Hum. Brain Mapp. 15 (2002) 95–111.
[28] X. Zhang, D.C. Hood, Increasing the sensitivity of the multifocal visual evoked potential (mfVEP) technique: incorporating information from higher order kernels using a principal component analysis method, Doc. Ophthalmol. 108 (3) (2004) 211–222.
[29] A. Capilla, M. Melcón, D. Kessel, R. Calderón, P. Pazo-Álvarez, L. Carretié, Retinotopic mapping of visual event-related potentials, Biol. Psychol. 118 (2016) 114–125.
[30] M.I. Sereno, A.M. Dale, J.B. Rappas, K.K. Kwong, J.W. Bellivau, T.J. Brady, B.R. Rosen, R.B.H. Tootell, Borders of multiple visual areas in humans revealed by functional magnetic resonance imaging, Science 268 (1995) 889–893.
[31] B.A. Wandell, S.O. Dumoulin, A.A. Brewer, Visual Field maps in human cortex, Neuron 56 (2) (2007) 366–383.
[32] J.M. Ales, T. Carney, S.A. Klein, The folding fingerprint of visual cortex reveals the timing of human V1 and V2, Neuroimage 49 (3) (2010) 2494–2502.
[33] G.R. Mangun, S.A. Hillyard, S.J. Luck, Electrophysiological substrates of visual selective attentiom, in: DE Meyer, S. Kornblum (Eds.), Attention and Performance XIV, The MIT Press, Cambridge, MA, 1993, pp. 219–243.
[34] S. Fu, M. Zinni, P.N. Squire, R. Kumar, D.M. Caggiano, R. Parasuraman, When and where perceptual load interacts with voluntary visuospatial attention: an event-related potential and dipole modelling study, Neuroimage 39 (2008) 1345–1355.
[35] G.L. Zhang, H. Li, Y. Song, C. Yu, ERP C1 is top-down modulated by orientation perceptual learning, J. Vis. 15 (8) (2015).
[36] V. Poghosian, A.A. Ioannides, Attention modulates earliest responses in the primary auditory and visual cortices, Neuron 58 (2008) 802–813.
[37] C.M. Karns, R.T. Knight, Intermodal auditory, visual, and tactile attention modulates early stages of neural processing, J. Cognit. Neurosci. 21 (2008) 669–683.
[38] A.A. Ioannides, V. Poghosian, Spatiotemporal dynamics of early spatial and category-specific attentional modulations, Neuroimage 60 (2012) 1638–1651.
[39] K.S. Rauss, G. Pourtois, P. Vuilleumier, S. Schwartz, Attentional load modifies activity in human primary visual cortex, Hum. Brain Mapp. 30 (2009) 1723–1733.
[40] S. Fu, Y. Huang, Y. Wang, J. Fedota, P.M. Greenwood, R. Parasuraman, Perceptual load interacts with involuntary attention at early processing stages: event-related potential studies, Neuroimage 48 (2009) 191–199.
[41] S. Fu, J.R. Fedota, P.M. Greenwood, R. Parasuraman, Dissociation of visual C1 and P1 components as a function of attentional load: an event-related potential study, Biol. Psychol. 85 (2010) 171–178.
[42] B.C. Motter, Focal attention produces spatially selective processing in visual cortical areas V1, V2, and V4 in the presence of competing stimuli, J. Neurophysiol. 70 (1993) 909–919.
[43] M. Ito, C.D. Gilbert, Attention modulates contextual influences in the primary visual cortex of alert monkey, Neuron 22 (1999) 593–604.
[44] C.J. McAdams, R.C. Reid, Attention modulates the responses of simple cells in monkey primary visual cortex, J. Neurosci. 25 (2005) 11023–11033.
[45] K. McAlonan, J. Cavanaugh, R.H. Wurtz, Guarding the gateway to cortex with attention in visual thalamus, Nature 456 (2008) 391–395.
[46] F. Briggs, G.R. Mangun, W.M. Ursey, Attention enhances synaptic efficacy and the signal-to-noise ratio in neural circuits, Nature 499 (7459) (2013) 476–480.
[47] Y. Ding, A. Martinez, Q. Zhe, S.A. Hillyard, Earliest stages of visual cortical processing are not modified by attentional load, Hum. Brain Mapp. 35 (2014) 3008–3024.
[48] H.M. Baumgartner, C.J. Graulty, S.A. Hillyard, M.A. Pitts, Does spatial attention modulate the C1 component? The jury continues to deliberate, Cognit. Neurosci. (2017a).
[49] S.D. Slotnick, The experimental parameters that affect attentional modulation oft he ERP C1 component, Cognit. Neurosci. (2017).

[50] S. Yamaguchi, H. Tsuchiya, S. Kobayashi, Electroencephalographic activity associated with shifts of visuospatial attention, Brain 117 (1994) 553–562.
[51] M. Eimer, Spatial cueing, sensory gating and selective response preparation: an ERP study on visuo-spatial orienting, EEG. Clin. Neurophysiol. 88 (1993) 408–420.
[52] J.-M. Hopf, G.R. Mangun, Shifting visual attention in space: an electrophysiological analysis using high spatial resolution mapping, Clin. Neurophysiol. 111 (2000) 1241–1257.
[53] A.C. Nobre, G.N. Sebestyen, C. Miniussi, The dynamics of shifting visuospatial attention revealed by event-related potentials, Neuropsychology 38 (2000) 964–974.
[54] M.C. Woldorff, C.j. Hazlett, H.M. Fichtenoltz, A. Weissman, A.M. Dale, A.W. Song, Functional parcellation of attentional control regions of the brain, J. Cognit. Neurosci. 16 (2004) 149–165.
[55] J. Grent-'T-Jong, M.G. Woldorff, Timing and sequence of brain activity in top-down control of visual-spatial attention, PLoS Biol. 5 (2007) 114–126.
[56] J. Fan, B.D. McCandliss, T. Sommer, A. Raz, M.I. Posner, Testing the efficiency and independence of attentional networks, J. Cognit. Neurosci. 14 (3) (2002) 340–347.
[57] R. Oostenveld, P. Praamstra, The five percent electrode system for high-resolution EEG and ERP measurements, Clin. Neurophysiol. 112 (2001) 713.
[58] A. Zani, A.M. Proverbio, in: J.R. Dupri (Ed.), ERP Signs of Frontal and Occipital Processing of Visual Targets and Distracters within and without the Channel of Spatial Attention. Focus on Neuropsychology Research, Nova Science Publishers, New York, 2006, pp. 38–88.
[59] R. Bakeman, Recommended effect size statistics for repeated measures designs, Behav. Res. Methods 37 (2005) 379–384.
[60] S. Olejnik, J. Algina, Generalized eta and omega squared statistics: measures of effect size for some common research designs, Psychol. Methods 8 (2003) 434–447.
[61] R.D. Pasqual-Marqui, C.M. Michel, D. Lehmann, Low resolution electromagnetic tomography: a new method for localizing electrical activity in the brain, J. Psychophysiol. 18 (1994) 49–65.
[62] E. Palmero-Soler, K. Dolan, V. Hadamschek, P.A. Tass, swLORETA: a novel approach to robust source localization and synchronization tomography, Phys. Med. Biol. 52 (2007) 1783–1800.
[63] D. Vitacco, D. Brandeis, R. Pascual-Marqui, E. Martin, Correspondence of event-related potential tomography and functional magnetic resonance imaging during language processing, Hum. Brain Mapp. 17 (2002) 4–12.
[64] B. Horwitz, D. Poeppel, How can EEG/MEG and fMRI/PET data be combined? Hum. Brain Mapp. 17 (1) (2002) 1–3.
[65] F. Zanow, T.R. Knösche, ASA-advanced source analysis of continuous and event-related EEG/MEG signals, Brain Topogr. 16 (4) (2004) 287.
[66] J. Tailarach, P. Tournoux, Co-planar Stereotaxic Atlas of the Human Brain, Thieme, New York, 1988.
[67] J.L. Lancaster, L.H. Rainey, J.L. Summerlin, C.S. Freitas, P.T. Fox, A.C. Evans, A.W. Toga, J.C. Mazziotta, Automated labeling of the human brain: a preliminary report on the development and evaluation of a forward-transform method, Hum. Brain Mapp. 5 (1997) 238–242.
[68] J.L. Lancaster, M.G. Woldorff, L.M. Parsons, M. Liotti, C.S. Freitas, L. Rainey, P.V. Kochunov, D. Nickerson, S.A. Mikiten, P.T. Fox, Automated Talairach Atlas labels for functional brain mapping, Hum. Brain Mapp. 10 (2000) 120–131.
[69] G.W. Snedecor, W.G. Cochran, Statistical Methods, eighth ed., Iowa State University Press: Iowa City, IA, , USA, 1989.
[70] L. Lison, Statistique Appliquée a la Biologie Experimentale. La Planification de L'expérience et L'analyse des Resultats, Gauthier-Villars Éditeur-Imprimeur-Libraire, Paris, France, 1961.
[71] S.S. Fukusima, J. Faubert, Perceived length in the central visual field: evidence for visual field asymmetries, Vis. Res. 41 (2001) 2119–2126.
[72] J. Feng, I. Spence, Upper visual field advantage in localizing a target among distractors, i-Percep 5 (2014) 97–100.
[73] A.M. Proverbio, M. Del Zotto, A. Zani, Inter-individual differences in the polarity of early visual responses and attention effects, Neurosci. Lett. 419 (2) (2007) 131–136.
[74] K. Anton-Erxleben, M. Carrasco, Attentional enhancement of spatial resolution: linking behavioural and neurophysiological evidence, Nat. Rev. Neurosci. 14 (3) (2013) 188–200.
[75] G. Pourtois, S. Delplanque, C. Michel, P. Vuilleumier, Beyond conventional event-related brain potential (ERP): exploring the time-course of visual emotion processing using topographic and principal component analyses, Brain Topogr. 20 (4) (2008) 265–277.
[76] J.J. Foxe, G. Simpson, Flow of activation from V1 to frontal cortex in humans. A framework for defining "early" visual processing, Exp. Brain Res. 142 (2002) 139–150.
[77] H.M. Baumgartner, C.J. Graulty, S.A. Hillyard, M.A. Pitts, Does spatial attention modulate the earliest component of the visual evoked potential? Cognit. Neurosci. (2018).
[78] J. Alilovic, B. Timmermans, L.G. Reteig, S. van Gaal, H.A. Slagter, No evidence that predictions and attention modulate the first feedforward sweep of cortical information processing, Cerebr. Cortex 29 (2019) 2261–2278.
[79] A. Zani, A.M. Proverbio, Endogenous attention to object features modulates the ERP C1 component, Cognit. Neurosci. 9 (1-2) (2018) 1–3. PMID: 29065816.
[80] F. Faul, E. Erdfelder, A.-G. Lang, B. Ag, G*Power 3: a flexible statistical power analysis program for the social, behavioral, and biomedical sciences, Behav. Res. Methods Instrum. Comput. 39 (2007) 175–191.